Available online at http://scik.org
J. Math. Comput. Sci. 2 (2012), No. 2, 339-359
ISSN: 1927-5307

TEMPERATURE RISE IN A TWO-LAYER STRUCTURE INDUCED BY A ROTATING OR DITHERING LASER BEAM

HONG ZHOU*

Department of Applied Mathematics, Naval Postgraduate School, Monterey, CA 93943

Abstract. We study the maximum temperature rise induced by a rotating or dithering Gaussian laser beam on a two-layer body. First, we derive semi-analytical solutions by solving the transient three-dimensional heat equation in a semi-infinite domain with insulating surface. Second, we provide numerical solutions for a two-layer structure in a finite domain. Our results show that the maximum temperature rise can be reduced significantly either by applying a thin layer of coating on the protected object or by moving the beam or equivalently the object.

Keywords: temperature rise; heat equation; two-layer structure; dithering or rotating Gaussian laser beam

2000 AMS Subject Classification: 35K05; 80A20

1. Introduction

Laser-induced heating plays an important role in materials processing [11]. The theoretical modeling of temperature profiles induced by laser radiation in solids has been extensively studied. For example, in [7] Lax modeled the spatial distribution of the temperature rise induced by a stationary Gaussian laser beam in a solid sample using a one-dimensional

*Corresponding author

E-mail address: hzhou@nps.edu(H.Zhou)

Received December 20, 2011

integral based on thermal conduction in the material. Since the closed-form solution in [7] is a steady state solution to the heat equation, it is limited to stationary or slow moving beams. Later Lax extended his analysis in [7] to allow temperature-dependent thermal conductivity [8]. Further theoretical and numerical developments include time-dependent solution for a scanning Gaussian beam [6], laser-melted front [3], continuous wave (cw) laser annealing of heterogeneous multilayer structures [5], temperature profiles induced by a moving cw elliptical laser beam with the inclusion of the temperature-dependent surface reflectivity and thermal diffusivity [9], a general analytic solution for the temperature rise produced by scanning Gaussian laser beams [12], the Green's function solution to the heat equation for a two-layer structure with scanning circular energy beams [4], the transient three-dimensional analytical solution of the temperature distribution in a finite solid when heated by a moving heat source [1], and the laser forming of plates using rotating or dithering Gaussian beams [13].

However, the main purpose of this paper is to find ways to reduce the maximum temperature rise induced by a laser beam, which is relevant to military applications. In [15] we have derived the analytical solution for the temperature rise induced by a rotating or dithering laser beam in a semi-infinite domain by solving a transient three-dimensional non-homogeneous heat equation. In [14] we have carried out numerical simulations to obtain the temperature rise induced by a rotating or dithering laser beam on a finite body. These studies have shown that the maximum temperature rise can be reduced by increasing the frequency of the rotating or dithering beam. In this paper we would like to extend our previous studies to a two-layer structure. In particular, we would like to investigate the effect of a thin layer of coating on the temperature rise induced by a laser beam.

We organize our presentation as follows. In Section 2 we derive semi-analytical solutions of the transient temperature distributions induced by a rotating or dithering laser beam in a semi-infinite domain. We present our numerical results for a finite domain in Section 3. Our main results are summarized in Section 4.

2. Semi-analytical solution in a semi-infinite domain

Consider a laser beam along the z direction, hitting a solid surface in the x-y plane and rotating in the x-y plane. The solid has a two-layer structure which consists of a film of thickness a in the z-direction (region 1) and a substrate of infinite thickness (region 2). The material of the solid is assumed to be isotropic and the solid is infinite in the x and y directions. Figure 1 depicts the geometries of the problem to be solved and the coordinate system that we have chosen. A semi-infinite geometry is a reasonably good approximation if the laser beam is small compared to the object. Heat loss from the target surface is assumed to be negligible compared to conduction into the solid.

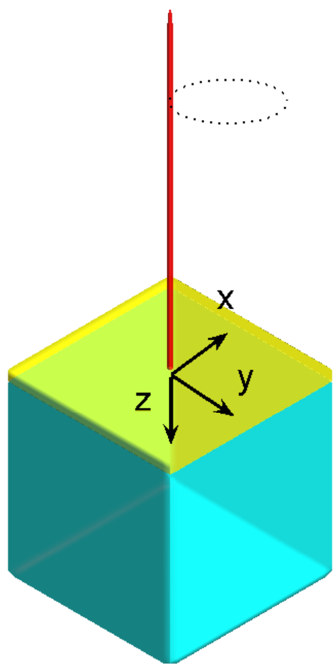

FIGURE 1. A schematic diagram shows a rotating laser beam on a two-layer object.

In general, the heat equation for an isotropic medium with a temperature-dependent thermal conductivity K can be written as

$$\frac{\partial T}{\partial t} - \frac{1}{\rho C}\nabla \cdot (K(T)\nabla T) = \frac{Q(x, y, z, t)}{\rho C}, \tag{1}$$

where $T(x,y,z,t)$ is the solid's temperature rise above ambient (i.e. the difference between the solid temperature and the ambient temperature) and it is a function of space (x,y,z) and time t, ∇ is the gradient operator, ρ is the density, C is the heat capacity, K is the thermal conductivity, and $Q(x,y,z,t)$ is the incident heat source term. The temperature-dependent thermal conductivity $K(T)$ can be removed from the heat equation by applying a Kirchhoff transformation.

The Kirchhoff transformation introduces a linearized temperature rise θ defined as

$$\theta(T) = \theta(T_0) + \int_{T_0}^{T} \frac{K(T')}{K(T_0)} dT', \quad \text{or} \quad \frac{d\theta}{dT} = \frac{K(T)}{K(T_0)}, \tag{2}$$

where $\theta(T_0)$ and $K(T_0)$ are constants. Note that when the thermal conductivity is constant, then (2) implies that $\theta(T) = T$ if we choose $\theta(T_0) = T_0$. Applying the chain rule, we have

$$\frac{\partial\theta}{\partial t} = \frac{d\theta}{dT}\frac{\partial T}{\partial t} = \frac{K(T)}{K(T_0)}\frac{\partial T}{\partial t}, \quad \text{or} \quad \frac{\partial T}{\partial t} = \frac{K(T_0)}{K(T)}\frac{\partial\theta}{\partial t}, \tag{3}$$

and

$$\nabla\theta = \frac{d\theta}{dT}\nabla T = \frac{K(T)}{K(T_0)}\nabla T, \quad \text{or} \quad \nabla T = \frac{K(T_0)}{K(T)}\nabla\theta. \tag{4}$$

Substituting the expressions (3) and (4) into the heat equation (1), we can express the heat equation (1) in terms of the linearized temperature rise θ as

$$\frac{\partial\theta}{\partial t} - D\Delta\theta = \frac{Q(x,y,z,t)D}{K(T_0)}, \tag{5}$$

where $D = K(\theta)/\rho C(\theta)$ is the thermal diffusivity of the material, and Δ is the Laplacian operator. Under the assumption of constant thermal diffusivity, equation (5) becomes a partial differential equation with constant coefficients.

For the two-layer structure depicted in Figure 1, the laser beam hits the surface $z = 0$. The linear heat equation for region 1 is

$$\frac{\partial\theta_1}{\partial t} - D_1\Delta\theta_1 = \frac{Q(x,y,z,t)D_1}{K_1(T_0)}, \tag{6}$$

and the linear heat equation for region 2 is

$$\frac{\partial\theta_2}{\partial t} - D_2\Delta\theta_2 = \frac{Q(x,y,z,t)D_2}{K_2(T_0)}, \tag{7}$$

where D_1, D_2 are the thermal diffusivities of the materials in region 1 and region 2, respectively. Initially the temperature rise is assumed to be zero. The boundary conditions for θ_1 and θ_2 are

$$\frac{\partial \theta_1}{\partial z} = 0 \ \text{ at } \ z = 0; \tag{8}$$

$$K_1(T)\frac{\partial \theta_1}{\partial z} = K_2(T)\frac{\partial \theta_2}{\partial z} \ \text{ at } \ z = a; \tag{9}$$

$$\theta_1 = \theta_2 \ \text{ at } \ z = a; \tag{10}$$

$$\theta_2 = 0 \ \text{ at } \ \text{infinity}. \tag{11}$$

The first boundary condition (8) imposes the insulating boundary condition at the air/material interface which assumes that no energy escapes into the air at the air/material interface. This is a reasonable approximation for most materials under consideration, since heat flow by conduction through the substrate far exceeds the loss by radiation or convection at the air/material interface. The second boundary condition (9) requires energy conservation for heat flow across the interface between regions 1 and 2. Here we have assumed that $K_1(T)/K_2(T) \equiv \alpha$ is a constant independent of temperature. This approximation can be met by many material combinations (e.g. silicon on sapphire). The third boundary condition (10) corresponds to temperature continuity at the interface between two regions, and the last boundary condition (11) implies that the temperature rise becomes zero at infinity, or equivalently, the temperature of the solid approaches the ambient temperature at infinity.

The energy absorbed in the top surface of region 1 ($z = 0$) is

$$Q(x, y, z, t) = \frac{3Q_0}{\pi r_0^2} \exp\left[-\frac{(x - a_1 \cos\frac{2\pi t}{s^*})^2 + (y + b_1 \sin\frac{2\pi t}{s^*})^2}{r_0^2/3}\right]\delta(z), \tag{12}$$

in the case of a rotating laser beam. Here Q_0 is the power absorbed and it is the product of the absorptivity and the laser power [13], r_0 is the characteristic beam radius typically defined as the radius at which the intensity of the laser beam drops to 5% of the maximum intensity, s^* is the rotating period. The Dirac delta function in z expresses the assumption that all the energy is absorbed at the surface. (12) describes a clockwise rotating beam in the x-y plane. If $a_1 = b_1$, then a_1 denotes the beam radius of the rotation along the z-axis. When $a_1 = 0$, (12) depicts the case of a dithering laser beam.

The general solution of (6) and (7) can be obtained by a Green's function method [2, 4]. Denote the Green's functions for regions 1 and 2 as G_1 and G_2, respectively. Then the Green's functions G_1 and G_2 satisfy

$$\frac{\partial G_1}{\partial t} - D_1 \Delta G_1 = -\delta(\vec{r} - \vec{r'})\delta(t - t'), \tag{13}$$

and

$$\frac{\partial G_2}{\partial t} - D_2 \Delta G_2 = 0, \tag{14}$$

where $|\vec{r} - \vec{r'}| = (x - x')^2 + (y - y')^2 + (z - z')^2$. The initial conditions are

$$G_1 = 0 \ \text{ at } \ t = t' \ \text{ for } \ \vec{r} \neq \vec{r'}; \quad G_2 = 0 \ \text{ at } \ t = t', \tag{15}$$

whereas the boundary conditions for G_1 and G_2 are the same as (8)-(9) with θ_1 replaced by G_1 and θ_2 replaced by G_2.

Following the work of [2, 4], one can express the Laplace transformed Green's functions as

$$\begin{aligned}
\bar{G_1} &= \frac{1}{2\pi D_1} \int_0^\infty \left[\exp(-\eta_1 z) + \frac{(\alpha\eta_1 - \eta_2)\exp(-\eta_1 a)\cosh(\eta_1 z)}{\alpha\eta_1 \sinh(\eta_1 a) + \eta_2 \cosh(\eta_1 a)} \right] \frac{\xi J_0(\xi R)}{\eta_1} d\xi \\
\bar{G_2} &= \frac{1}{2\pi D_1} \int_0^\infty \left[\exp(-\eta_2 z) + \frac{(\alpha\eta_1 - \eta_2)\exp(-\eta_2 z)\cosh(\eta_1 a)}{\alpha\eta_1 \sinh(\eta_1 a) + \eta_2 \cosh(\eta_1 a)} \right] \\
&\quad \times \exp[a(\eta_2 - \eta_1)] \frac{\xi J_0(\xi R)}{\eta_1} d\xi
\end{aligned} \tag{16}$$

where $\bar{G_1}$ and $\bar{G_2}$ are the Laplace transforms of G_1 and G_2, respectively:

$$\bar{G_i} \equiv \int_0^\infty \exp[-p(t - t')] G_i d(t - t'), \ i = 1, 2, \tag{17}$$

and J_0 is the Bessel function of tbe first kind or order zero,

$$\begin{aligned}
\eta_i &= \sqrt{\xi^2 + \tfrac{p}{D_i}}, \ i = 1, 2, \\
R &= \sqrt{(x - x')^2 + (y - y')^2}, \\
\alpha &= K_1(T)/K_2(T) = \text{constant}.
\end{aligned} \tag{18}$$

In the appendix we verify that the expressions of $\bar{G_1}$ and $\bar{G_2}$ in (16) are correct.

With the help of the three-dimensional Green's function, the solution of the inhomogeneous heat equations (6) and (7) for a semi-infinite medium can be expressed as

$$\begin{aligned} \theta_1(x,y,z,t) &= \frac{3Q_0}{2\pi^2 r_0^2 D_1 K_1(T_0)} \int_{-\infty}^{t}\int_{-\infty}^{\infty}\int_{-\infty}^{\infty}\int_{0}^{\infty}\int_{\delta-i\infty}^{\delta+i\infty} \frac{\exp[p(t-t')]}{2\pi i} \\ &\times \left[\exp(-\eta_1 z) + \frac{(\alpha\eta_1-\eta_2)\exp(-\eta_1 a)\cosh(\eta_1 z)}{\alpha\eta_1\sinh(\eta_1 a)+\eta_2\cosh(\eta_1 a)}\right] \frac{\xi J_0(\xi\sqrt{(x-x')^2+(y-y')^2})}{\eta_1} \\ &\times \exp\left[-\frac{(x'-a_1\cos\frac{2\pi t'}{s^*})^2+(y'+b_1\sin\frac{2\pi t'}{s^*})^2}{r_0^2/3}\right] dp\, d\xi\, dy'\, dx'\, dt' \end{aligned} \tag{19}$$

for region 1 and

$$\begin{aligned} \theta_2(x,y,z,t) &= \frac{3Q_0}{2\pi^2 r_0^2 D_1 K_2(T_0)} \int_{-\infty}^{t}\int_{-\infty}^{\infty}\int_{-\infty}^{\infty}\int_{0}^{\infty}\int_{\delta-i\infty}^{\delta+i\infty} \frac{\exp[p(t-t')]}{2\pi i} \\ &\times \left[\exp(-\eta_2 z) + \frac{(\alpha\eta_1-\eta_2)\exp(-\eta_2 z)\cosh(\eta_1 a)}{\alpha\eta_1\sinh(\eta_1 a)+\eta_2\cosh(\eta_1 a)}\right] \exp[a(\eta_2-\eta_1)] \frac{\xi J_0(\xi\sqrt{(x-x')^2+(y-y')^2})}{\eta_1} \\ &\times \exp\left[-\frac{(x'-a_1\cos\frac{2\pi t'}{s^*})^2+(y'+b_1\sin\frac{2\pi t'}{s^*})^2}{r_0^2/3}\right] dp\, d\xi\, dy'\, dx'\, dt' \end{aligned} \tag{20}$$

for region 2.

The formulas in both (19) and (20) involve quintuple integrals. In order to reduce them to expressions with double integrals, we apply the same procedure as in [4]. First, we consider the integral over x' and y'in (19) which is denoted as I_1:

$$\begin{aligned} I_1 &= \int_{-\infty}^{\infty}\int_{-\infty}^{\infty} J_0\left(\xi\sqrt{(x-x')^2+(y-y')^2}\right) \\ &\times \exp\left[-\frac{(x'-a_1\cos\frac{2\pi t'}{s^*})^2+(y'+b_1\sin\frac{2\pi t'}{s^*})^2}{r_0^2/3}\right] dy'\, dx' \end{aligned} \tag{21}$$

Introducing the new independent variables $X = x - x'$ and $Y = y - y'$ into (21), we obtain

$$\begin{aligned} I_1 &= \int_{-\infty}^{\infty}\int_{-\infty}^{\infty} J_0\left(\xi\sqrt{X^2+Y^2}\right) \\ &\times \exp\left[-\frac{(X - x + a_1\cos\frac{2\pi t'}{s^*})^2 + (Y - y - b_1\sin\frac{2\pi t'}{s^*})^2}{r_0^2/3}\right] dY\,dX \\ &= \int_{-\infty}^{\infty}\int_{-\infty}^{\infty} J_0\left(\xi\sqrt{X^2+Y^2}\right)\exp\left[-\frac{\|\vec{R}_{ab}-\vec{L}\|^2}{r_0^2/3}\right] dY\,dX. \end{aligned} \tag{22}$$

Here $\vec{R}_{ab} = (x - a_1\cos\frac{2\pi t'}{s^*})\vec{i} + (y + b_1\sin\frac{2\pi t'}{s^*})\vec{j}$ and $\vec{L} = X\vec{i} + Y\vec{j}$. It is convenient to write (22) in polar coordinates:

$$\begin{aligned} I_1 &= \int_0^{\infty}\int_0^{2\pi} J_0(\xi L)\exp\left[-\frac{R_{ab}^2 + L^2 - 2R_{ab}L\cos\phi}{r_0^2/3}\right] L d\phi\,dL \\ &= 2\pi\int_0^{\infty} J_0(\xi L) I_0(\frac{2R_{ab}L}{r_0^2/3})\exp\left[-\frac{R_{ab}^2+L^2}{r_0^2/3}\right] L\,dL, \end{aligned} \tag{23}$$

where $R_{ab}^2 = (x - a_1\cos\frac{2\pi t'}{s^*})^2 + (y + b_1\sin\frac{2\pi t'}{s^*})^2$, $L^2 = X^2 + Y^2$ and I_0 is the modified Bessel function of the first kind defined by $I_0(z) = \frac{1}{\pi}\int_0^{\pi}\exp[z\cos\theta]d\theta$.

In order to reduce (23) further, we employ an identity from [10] (Page 963, Eq. (8.5.10) and Eq. (a)):

$$\frac{1}{2p^2}\exp\left[-\frac{x^2+x_0^2}{4p^2}\right] I_0(\frac{xx_0}{2p^2}) = \int_0^{\infty} J_0(kx)\exp[-p^2k^2] J_0(kx_0)kdk. \tag{24}$$

Introducing $x = L$, $x_0 = R_{ab}$ and $p^2 = r_0^2/12$ into (24), we obtain

$$\exp\left[-\frac{L^2+R_{ab}^2}{r_0^2/3}\right] I_0(\frac{2R_{ab}L}{r_0^2/3}) = \frac{r_0^2}{6}\int_0^{\infty} J_0(kL)\exp[-r_0^2k^2/12] J_0(kR_{ab})kdk. \tag{25}$$

Inserting (25) back in (23) ,we find

$$I_1 = \frac{\pi r_0^2}{3}\int_0^{\infty}\int_0^{\infty} J_0(\xi L)J_0(kL)J_0(kR_{ab})k\exp\left[-\frac{k^2r_0^2}{12}\right] L\,dL\,dk. \tag{26}$$

Substituting the orthogonality property of Bessel functions (also called the *closure equation*)

$$\int_0^{\infty} LJ_0(kL)J_0(\xi L)dL = \frac{1}{\sqrt{k\xi}}\delta(k-\xi) = \frac{1}{k}\delta(k-\xi), \tag{27}$$

in (26) yields

$$I_1 = \frac{\pi r_0^2}{3} \int_0^\infty \delta(k-\xi) J_0(kR_{ab}) \exp\left[-\frac{k^2 r_0^2}{12}\right] dk = \frac{\pi r_0^2}{3} J_0(\xi R_{ab}) \exp\left[-\frac{\xi^2 r_0^2}{12}\right]. \tag{28}$$

We may now return to (19). The linear heat rise in region 1 can be written as

$$\begin{aligned} \theta_1(x,y,z,t) &= \frac{Q_0}{4\pi^2 i D_1 K_1(T_0)} \int_{-\infty}^{t} \int_0^\infty \int_{\delta-i\infty}^{\delta+i\infty} \exp[p(t-t')] \\ &\times \left[\exp(-\eta_1 z) + \frac{(\alpha\eta_1 - \eta_2)\exp(-\eta_1 a)\cosh(\eta_1 z)}{\alpha\eta_1 \sinh(\eta_1 a) + \eta_2 \cosh(\eta_1 a)}\right] \\ &\times \frac{\xi\, J_0(\xi R_{ab})}{\eta_1} \exp\left[-\frac{\xi^2 r_0^2}{12}\right] dp\, d\xi\, dt' \end{aligned} \tag{29}$$

In [4] a scanning laser beam was used and the steady state solution was studied. With the help of the residue theorem one was able to find the integral with respect to the variable p and thereby reduce the triple integral to a double integral. Here a rotating or dithering laser beam is considered and we are interested in time-dependent solution. As a result, the techniques used in [4] cannot be extended here.

Now making a change of variables $\bar{t} = t - t'$, we can rewrite (29) as

$$\begin{aligned} \theta_1(x,y,z,t) &= \frac{Q_0}{4\pi^2 i D_1 K_1(T_0)} \int_0^\infty \int_0^\infty \int_{\delta-i\infty}^{\delta+i\infty} \exp[p\bar{t}] \\ &\times \left[\exp(-\eta_1 z) + \frac{(\alpha\eta_1 - \eta_2)\exp(-\eta_1 a)\cosh(\eta_1 z)}{\alpha\eta_1 \sinh(\eta_1 a) + \eta_2 \cosh(\eta_1 a)}\right] \\ &\times \frac{\xi\, J_0(\xi \bar{R}_{ab})}{\eta_1} \exp\left[-\frac{\xi^2 r_0^2}{12}\right] dp\, d\xi\, d\bar{t} \\ &= \frac{Q_0}{2\pi D_1 K_1(T_0)} \int_0^\infty \int_0^\infty \xi\, J_0(\xi \bar{R}_{ab}) \exp\left[-\frac{\xi^2 r_0^2}{12}\right] F_1(\bar{t},\xi) d\xi\, d\bar{t}, \end{aligned} \tag{30}$$

where $\bar{R}_{ab}^2 = (x - a_1 \cos\dfrac{2\pi(t-\bar{t})}{s^*})^2 + (y + b_1 \sin\dfrac{2\pi(t-\bar{t})}{s^*})^2$, $F_1(\bar{t},\xi)$ is the inverse Laplace transform of a complicated function given explicitly by

$$F_1(\bar{t},\xi) = \frac{1}{2\pi i} \int_{\delta-i\infty}^{\delta+i\infty} \exp[p\bar{t}] \left[\exp(-\eta_1 z) + \frac{(\alpha\eta_1 - \eta_2)\exp(-\eta_1 a)\cosh(\eta_1 z)}{\alpha\eta_1 \sinh(\eta_1 a) + \eta_2 \cosh(\eta_1 a)}\right] \frac{1}{\eta_1} dp, \tag{31}$$

and recall that $\eta_i = \sqrt{\xi^2 + p/D_i}, i = 1, 2$.

In a similar fashion, the temperature for region 2 can be expressed in the form

$$\theta_2(x,y,z,t) = \frac{Q_0}{2\pi D_1 K_2(T_0)} \int_0^\infty \int_0^\infty \xi\, J_0(\xi \bar{R}_{ab}) \exp\left[-\frac{\xi^2 r_0^2}{12}\right] F_2(\bar{t},\xi) d\xi\, d\bar{t}, \tag{32}$$

where $F_2(\bar{t},\xi)$ is the inverse Laplace transform

$$F_2(\bar{t},\xi) = \frac{1}{2\pi i}\int_{\delta-i\infty}^{\delta+i\infty} \exp[p\bar{t}]\left[\exp(-\eta_2 z) + \frac{(\alpha\eta_1-\eta_2)\exp(-\eta_2 z)\cosh(\eta_1 a)}{\alpha\eta_1\sinh(\eta_1 a)+\eta_2\cosh(\eta_1 a)}\right] \times\frac{\exp[a(\eta_2-\eta_1)]}{\eta_1}dp. \tag{33}$$

The analytical solutions above involve the inverse Laplace transform and multiple integrals and thus it is numerically difficult to obtain meaningful solutions. As a future work we will try to simplify the expressions. In the next section we will solve the heat equations directly in a finite domain.

3. Numerical solutions in a finite domain

In this section we use the commerical software COMSOL to solve the heat equations directly for a two-layer structure in a finite domain. In the simulations below we model a two-layer structure where the substrate is made of aluminum and the thin coating layer is made of copper.

Figure 2 depicts the model geometry for a two-layer structure. It consists of a substrate made of one material and a thin layer of coating of different material. Ideally the coating materials should have larger thermal conductivity than the substrate materials. We assume that there is no energy escaping into the ambient at the air/structure interface so the boundaries are treated as insulating boundaries. For most situations this is a reasonable assumption since heat loss by radiation or convection at the interface is often much smaller than heat flow by conduction through the material. Furthermore, the structure is assumed to have the same temperature as the ambient initially so the initial temperature rise is set to zero.

For all the computations presented in this paper, we choose aluminum as the substrate material and copper as the coating material. Their thermal properties are listed in Table 1. For laser beams described in (12) we choose $Q_0 = 1.0\times10^5 W/m^2$, $r_0/\sqrt{6} = 0.02m$, $s^* = 1s$, $a_1 = 0.25m$, $b_1 = 0m$ (for a dithering laser beam), $b_1 = 0.25m$ (for a rotating laser

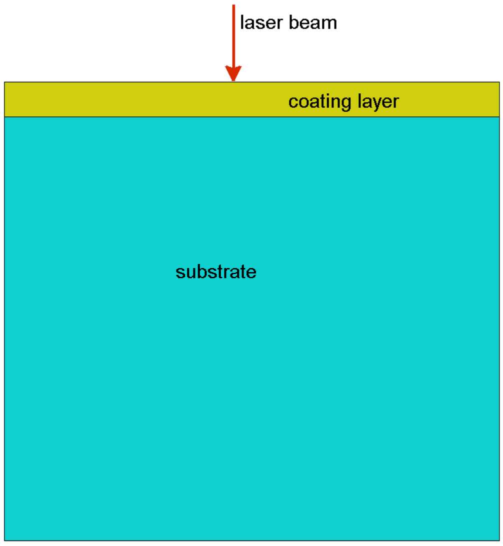

FIGURE 2. A plot of a two-dimensional two-layer structure.

beam). The two-layer structure is a three-dimensional box with dimension $1m \times 1m \times 1m$ and the center of the laser beam hits the center of the top surface.

Table 1: Thermal properties of copper and aluminum

Property Name	Copper	Aluminum
specific heat $(J/(kg \cdot K))$	385	900
thermal conductivity $(W/(m \cdot K))$	400	160
thermal diffusivity (m^2/s)	1.1942×10^{-4}	6.5844×10^{-5}
melting point (K)	1356	933
density (kg/m^3)	8700	2700

In Figure 3(a) we plot the temperature rise in an aluminum box induced by a Gaussian beam at time $= 1s$ whereas Figure 3(b) shows the temperature rise on a horizontal slice of Figure 3(a) through $z = 0.99m$. The maximum temperature $(1609K)$ is reached at the top surface where the beam hits the box. The maximum temperature rise drops to $937K$ at the horizontal slice $0.01m$ below the top surface. Figure 3(c) shows the temperature rise in an aluminum box coated with 0.1% thin copper layer on the top surface. The maximum temperature rise falls to $1352K$, which is about 16% reduction from the case without coating. Figure 3(d) depicts the corresponding temperature rise at the horizontal slice $0.01m$ below the top surface. Now the maximum temperature is reduced to $797K$.

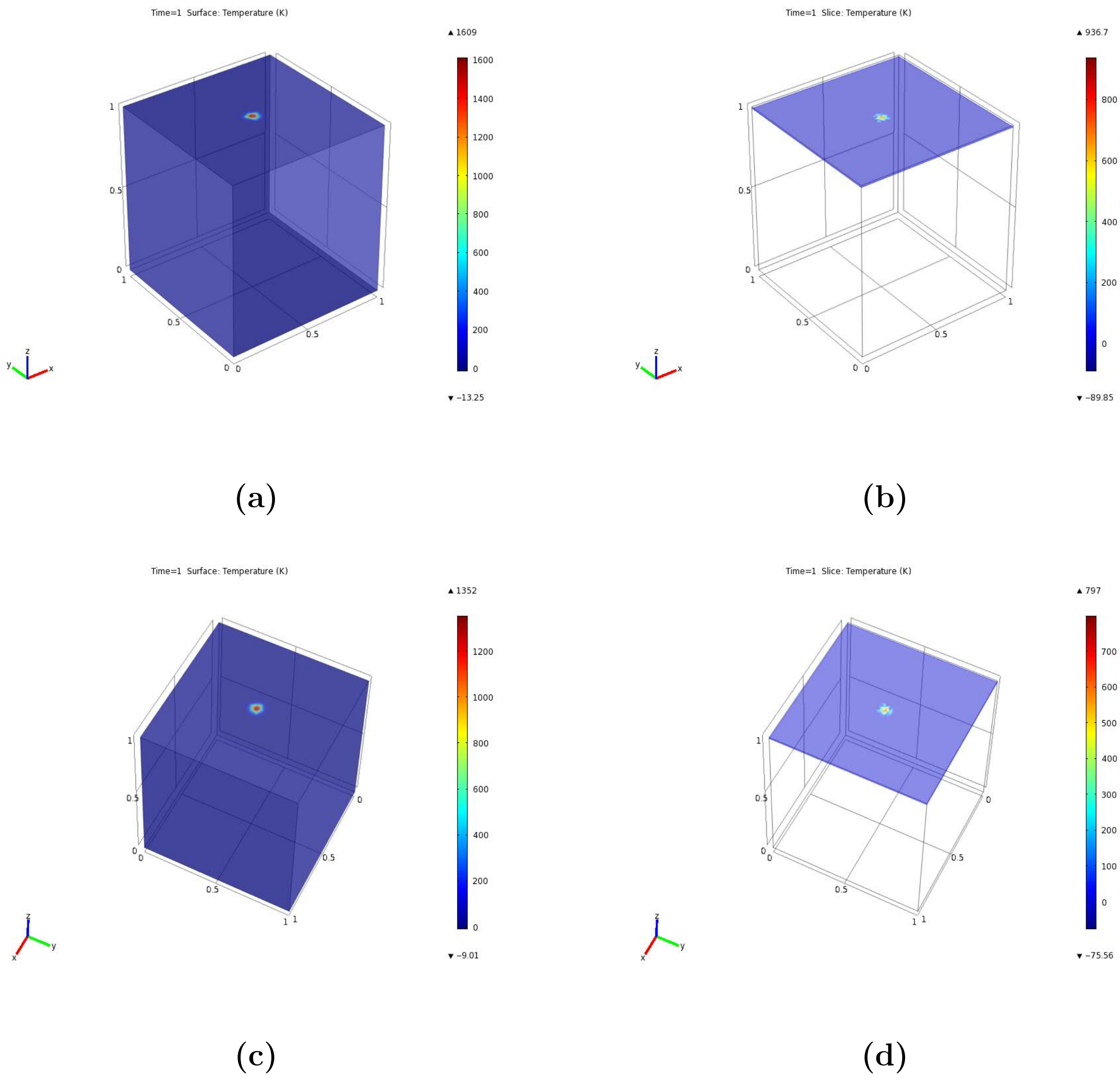

FIGURE 3. (a) Temperature rise of an aluminum box induced by a Gaussian beam with no coating; (b) a horizontal slice of part (a) through $z = 0.99$; (c) Temperature rise of an aluminum box with 0.1% copper skin on the top surface; (d) a horizontal slice of part (c) through $z = 0.99$

Figure 4(a) shows further the dependence of the maximum temperature rise of the two-layer box on the thickness of the coating layer. As expected, the maximum temperature rise decreases when the thickness of the coating layer increases. Figure 4(b) predicts the asymptotic behavior of the maximum temperature rise (in K) as a function of the thickness of the coating layer (in mm) using the least squares fitting:

$$T_{max} = \frac{-3290.32}{a^2} + \frac{3459.76}{a} + 252.79. \tag{34}$$

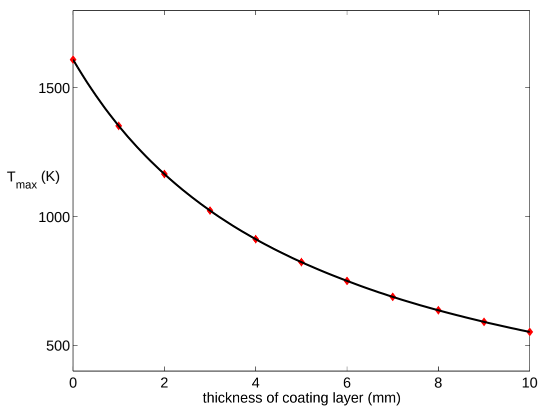

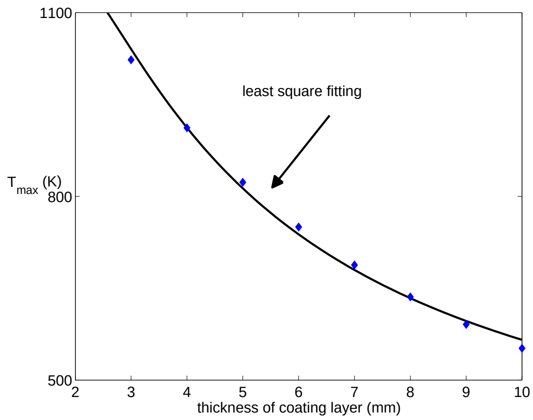

(a) **(b)**

Figure 4. (a)The maximum temperature rise of the two-layer aluminum box induced by a Gaussian beam as a function of the thickness of the copper coating layer. The computed data are represented by the red diamonds whereas the solid curve is obtained by a cubic spline interpolation. (b)The asymptoic behavior of the maximum temperature temperature rise (T_{max}) as a function of the thickness of the coating layer (a). The solid curve corresponds to the least squares fitting function $T_{max} = \frac{-3290.32}{a^2} + \frac{3459.76}{a} + 252.79$.

Next we let the laser beam dither or rotate and study the effect on the maximum temperature rise. We first apply a dithering Gaussian beam on the top surface of the aluminum box without coating and the temperature rise is depicted in Figure 5(a). Then we apply the same dithering Gaussian beam on the top surface of the aluminum box coated with 0.1% thin copper layer on the top surface. The corresponding temperature rise is shown in Figure 5(b). Due to the effect of the dithering beam the maximum temperature rise falls to $329K$ and it is further reduced to $268K$ if a thin layer (0.1%) of coating is applied. For the model case considered here, moving beam is more efficient than coating in reducing maximum temperature rise.

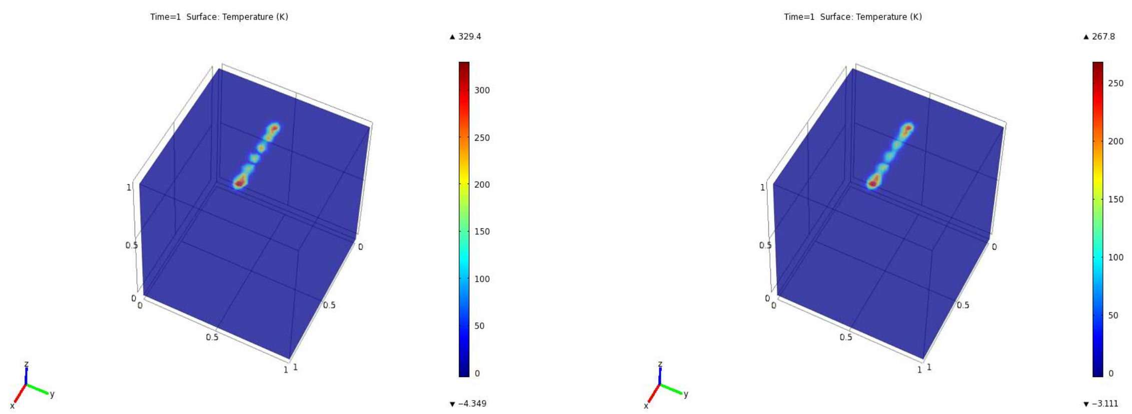

(a) **(b)**

FIGURE 5. (a)The maximum temperature rise of an aluminum box induced by a dithering Gaussian beam. (b)The maximum temperature rise due to a dithering Gaussian beam on an aluminum box coated with 0.1% copper layer.

Figure 6 is similar to Figure 5, but for a rotating Gaussian beam. The maximum temperature rise induced by a rotating beam is smaller than the one induced by a dithering beam.

The dependence of the maximum temperature rise on the thickness of the coating layer induced by a dithering or rotating laser beam is demonstrated in Figure 7(a) and (b) respectively together with least squares fitting curves. Figure 7(a) shows that for a dithering beam the maximum temperature rise depends on the thickness of the coating

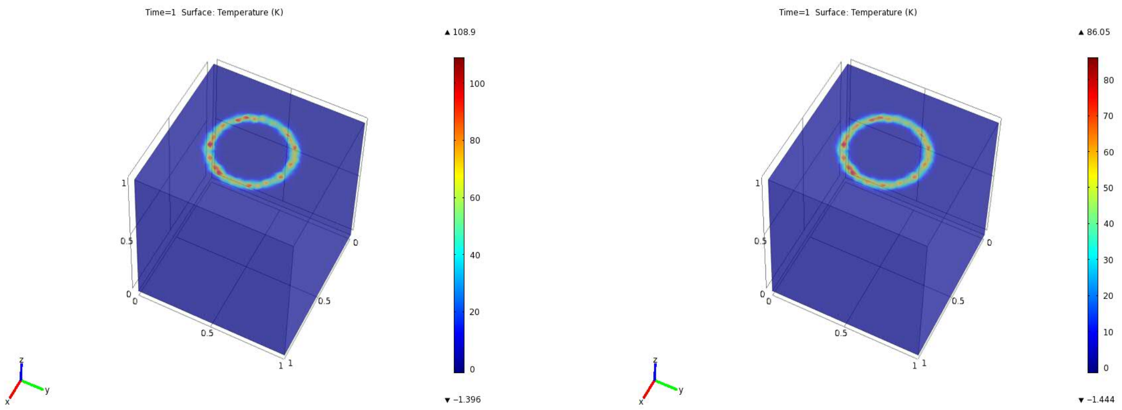

(a) **(b)**

FIGURE 6. (a)The maximum temperature rise of an aluminum box induced by a rotating Gaussian beam. (b)The maximum temperature rise due to a rotating Gaussian beam on an aluminum box coated with 0.1% copper layer.

layer as a function

$$T_{max} = \frac{-15.5595}{a^2} + \frac{72.7360}{a} + 210.9354, \tag{35}$$

whereas for a rotating beam the dependence is different:

$$T_{max} = \frac{-5.9499}{a^2} + \frac{28.0879}{a} + 64.0152, \tag{36}$$

as shown in Figure 7(b).

Finally, for comparison purpose, we summarize the results of Figures 3, 5 and 6 in Table 2 which shows quantitatively how the maximum temperature rise can be reduced for various cases. From Table 2, we summarize our observations: (1) rotating an object reduces the maximum temperature rise more than dithering the object; (2) moving an object is more efficient than coating in reducing maximum temperature rise. Finally, it is obvious from Table 2 that the most effective way to reduce the maximum temperature rise is to combine coating with a rotating Gaussian beam. From a practical defense point of view, this implies that in order to reduce the maximum temperature rise in an object

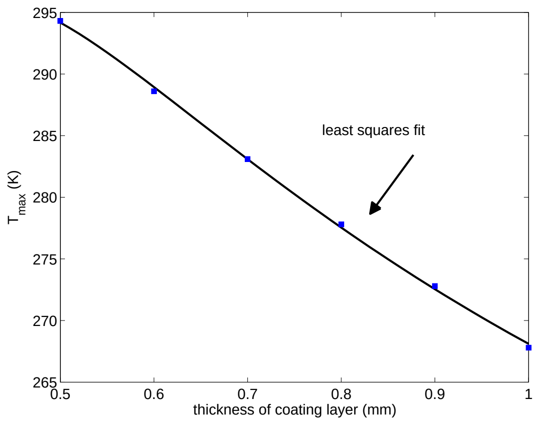

(a)

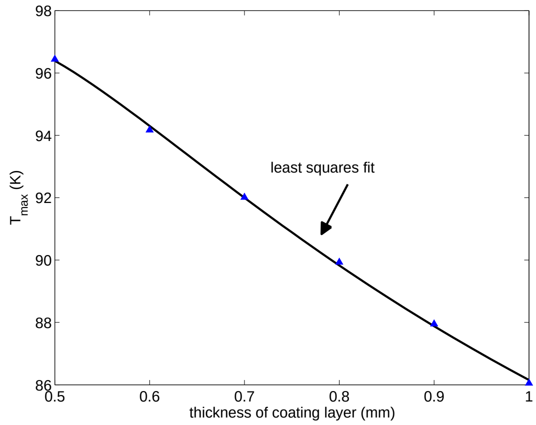

(b)

FIGURE 7. The maximum temperature rise of the two-layer aluminum box as a function of the thickness of the copper coating layer. The computed data are represented by symbols whereas the solid curves are obtained by the least squares approach. (a) The beam is a dithering Gaussian beam and the fitting function is $T_{max} = \frac{-15.5595}{a^2} + \frac{72.7360}{a} + 210.9354$. (b) The beam is a rotating Gaussian beam and the fitting function is $T_{max} = \frac{-5.9499}{a^2} + \frac{28.0879}{a} + 64.0152$.

hit by a laser beam, one possible way to protect the object is to apply a thin layer of coating materials on the object and also rotate the object.

Table 2: Summary of maximum temperature rise in various cases

	Gaussian beam	Dithering Gaussian beam	Rotating Gaussian beam
$T_{\max}^{\text{no coating}}$	1609	329	109
(K)	(reference temperature)	(79.55% reduction)	(93.23% reduction)
$T_{\max}^{0.1\%\text{ coating}}$	1352	268	86
(K)	(15.97% reduction)	(83.34% reduction)	(94.66% reduction)

4. Conclusions

In this paper we have derived the temperature rise induced by a rotating or dithering Gaussian laser beam for a semi-infinite two-layer structure. Numerical solutions for a finite two-layer structure are provided using COMSOL. It is found that the maximum temperature rise can be reduced significantly by applying a thin layer of coating or by moving the beam (or object).

Acknowledgment

We wish to thank Mr. Peter Morrison and the Office of Naval Research (ONR) for supporting this effort.

References

[1] G. Araya and G. Gutierrez, Analytical solution for a transient, three-dimensional temperature distribution due to a moving laser beam, Int. J. Heat and Mass Transfer 49 (2006), 4124-4131.

[2] R. Bellman, R.E. Marshak, and G.M. Wing, Laplace transform solution of two-medium neutron ageing problem, Philosophical Magazine Series 40(302) (1949), 297-308.

[3] M. Bertolotti and C. Sibilia, Depth and velocity of the laser-melted front from an anlytical solution of the heat conduction equation, IEEE J. Quantum Electron. QE-17 (1981), 1980-1989.

[4] M. L. Burgener and R. E. Reedy, Temperature distributions produced in a two-layer structure by a scanning cw laser or electron beam, J. Appl. Phys. 53 (1982), 4357-4363.

[5] I. D. Calder and R. Sue, Modeling of cw laser annealing of multilayer structures, J. Appl. Phys. 53 (1982), 7545-7550.

[6] H. E. Cline and T. R. Anthony, Heat treating and melting material with a scanning laser or electron beam, J. Appl. Phys. 48 (1977), 3895-3900.

[7] M. Lax, Temperature rise induced by a laser beam, J. Appl. Phys. 48 (1977), 3919-3924.

[8] M. Lax, Temperature rise induced by a laser beam II. The nonlinear case, Appl. Phys. Lett. 33(1978), 786-788.

[9] J. E. Moody and R. H. Hendel, Temperature profiles induced by a scanning cw laser beam, J. Appl. Phys. 53 (1982), 4364-4371.

[10] P.M. Morse and H. Feshbach, *Methods of Theoretical Physics*, Part I, McGraw-Hill, New York, 1953.

[11] J. Ready, Material Processing – An Overview, Proc. IEEE 70 (1982), 533-544.

[12] D. J. Sanders, Temperature distributions produced by scanning Gaussian laser beams, Applied Optics 23 (1984), 30-35.

[13] Me. Sistaninia, Ma. Sistaninia and H. Moeanodini, Laser forming of plates using rotating and dithering beams, Computational Materials Science 45 (2009), 480-488.

[14] T. Tan and H. Zhou, Numerical solution for a transient temperature distribution on a finite domain due to a dithering or rotating laser beam, International Journal of Operations Research and Information Systems, in press.

[15] H. Zhou, Temperature rise induced by a rotating or dithering laser beam, Advanced Studies in Theoretical Physics 5(10) (2011), 443-468.

Appendix. Verification of the Green Functions

In this appendix we verify that the Lapace tranformed Green functions in (16) are correct. For simplicity we consider only the case $\vec{r'} = \vec{0}$ (otherwise one can make a shift to obtain this case).

First, we check the expression of $\bar{G}_1$. Taking the Laplace transform of (13) and using the initial condition (15), we have an equation for $\bar{G}_1$:

$$p\bar{G}_1 - D_1 \Delta \bar{G}_1 = \delta(\vec{r} - \vec{r'}). \tag{37}$$

Using the cylindrical coordiates, we can express (37) explicitly as

$$p\bar{G}_1 - D_1 \left(\frac{\partial^2 \bar{G}_1}{\partial R^2} + \frac{1}{R}\frac{\partial \bar{G}_1}{\partial R} + \frac{\partial^2 \bar{G}_1}{\partial z^2} \right) = \delta(\vec{r}). \tag{38}$$

We consider the case where $\vec{r} \neq \vec{0}$. For $\bar{G}_1$ given in (16), it is straightforward to obtain that

(39)

$$\frac{\partial \bar{G}_1}{\partial R} = \frac{1}{2\pi D_1}\int_0^\infty \left[\exp(-\eta_1 z) + \frac{(\alpha\eta_1 - \eta_2)\exp(-\eta_1 a)\cosh(\eta_1 z)}{\alpha\eta_1\sinh(\eta_1 a) + \eta_2\cosh(\eta_1 a)}\right]\frac{\xi}{\eta_1}\frac{\partial J_0(\xi R)}{\partial R}d\xi$$

$$\frac{\partial^2 \bar{G}_1}{\partial R^2} = \frac{1}{2\pi D_1}\int_0^\infty \left[\exp(-\eta_1 z) + \frac{(\alpha\eta_1 - \eta_2)\exp(-\eta_1 a)\cosh(\eta_1 z)}{\alpha\eta_1\sinh(\eta_1 a) + \eta_2\cosh(\eta_1 a)}\right]\frac{\xi}{\eta_1}\frac{\partial^2 J_0(\xi R)}{\partial R^2}d\xi$$

$$\frac{\partial^2 \bar{G}_1}{\partial z^2} = \frac{1}{2\pi D_1}\int_0^\infty \left[\exp(-\eta_1 z) + \frac{(\alpha\eta_1 - \eta_2)\exp(-\eta_1 a)\cosh(\eta_1 z)}{\alpha\eta_1\sinh(\eta_1 a) + \eta_2\cosh(\eta_1 a)}\right]\eta_1^2\frac{\xi}{\eta_1}J_0(\xi R)d\xi$$

$$= \frac{1}{2\pi D_1}\int_0^\infty \left[\exp(-\eta_1 z) + \frac{(\alpha\eta_1 - \eta_2)\exp(-\eta_1 a)\cosh(\eta_1 z)}{\alpha\eta_1\sinh(\eta_1 a) + \eta_2\cosh(\eta_1 a)}\right]\xi^2\frac{\xi}{\eta_1}J_0(\xi R)d\xi + \frac{p}{D_1}\bar{G}_1$$

Thus, we have

$$
\begin{aligned}
& p\bar{G}_1 - D_1\left(\frac{\partial^2 \bar{G}_1}{\partial R^2} + \frac{1}{R}\frac{\partial \bar{G}_1}{\partial R} + \frac{\partial^2 \bar{G}_1}{\partial z^2}\right) \\
& = -\frac{1}{2\pi}\int_0^\infty \left[\exp(-\eta_1 z) + \frac{(\alpha\eta_1 - \eta_2)\exp(-\eta_1 a)\cosh(\eta_1 z)}{\alpha\eta_1\sinh(\eta_1 a) + \eta_2\cosh(\eta_1 a)}\right]\frac{\xi}{\eta_1} \\
& \quad \times \left[\frac{\partial^2 J_0(\xi R)}{\partial R^2} + \frac{1}{R}\frac{\partial J_0(\xi R)}{\partial R} + \xi^2 J_0(\xi R)\right] d\xi
\end{aligned} \tag{40}
$$

Introducing a new variable $s = \xi R$, we get

$$
\begin{aligned}
& J_0(\xi R) \equiv J_0(s), \\
& \frac{dJ_0}{ds} = \frac{\partial J_0}{\partial R}\frac{\partial R}{\partial s} = \frac{1}{\xi}\frac{\partial J_0}{\partial R}, \\
& \frac{d^2 J_0}{ds^2} = \frac{1}{\xi^2}\frac{\partial^2 J_0}{\partial R^2}.
\end{aligned} \tag{41}
$$

It follows immediately that

$$
\frac{\partial^2 J_0(\xi R)}{\partial R^2} + \frac{1}{R}\frac{\partial J_0(\xi R)}{\partial R} + \xi^2 J_0(\xi R) = \frac{1}{R^2}\left[s^2 J_0^{''}(s) + sJ_0^{'}(s) + s^2 J_0(s)\right] = 0 \tag{42}
$$

where in the last step we have used the fact that J_0 is the Bessel equation of order zero. Substituing (42) in Eq. (40), we obtain, finally,

$$
p\bar{G}_1 - D_1\Delta\bar{G}_1 = 0 \text{ for } \vec{r} \neq \vec{0}. \tag{43}
$$

In a similar way one can confirm that $\bar{G}_2$ satisfies

$$
p\bar{G}_2 - D_2\Delta\bar{G}_2 = 0. \tag{44}
$$

Finally, we check the boundary conditions.

$$
\frac{\partial \bar{G}_1}{\partial z} = \frac{1}{2\pi D_1}\int_0^\infty \left[-\exp(-\eta_1 z) + \frac{(\alpha\eta_1 - \eta_2)\exp(-\eta_1 a)\sinh(\eta_1 z)}{\alpha\eta_1\sinh(\eta_1 a) + \eta_2\cosh(\eta_1 a)}\right]\xi J_0(\xi R) d\xi \tag{45}
$$

This gives

$$
\frac{\partial \bar{G}_1}{\partial z}|_{z=0} = -\frac{1}{2\pi D_1}\int_0^\infty \xi J_0(\xi R) d\xi = -\frac{1}{2\pi D_1 R^2}\int_0^\infty sJ_0(s) ds, \tag{46}
$$

where we have made a change of variables $s = \xi R$. Since $J_0(s)$ satisfies Bessel's equation of order zero, we have

$$
s^2 J_0^{''}(s) + sJ_0^{'} + s^2 J_0(s) = 0, \tag{47}
$$

or,

$$sJ_0(s) = -[sJ_0''(s) + J_0'(s)] = -\frac{d}{ds}[sJ_0'(s)]. \tag{48}$$

Applying this result to $\frac{\partial \bar{G}_1}{\partial z}|_{z=0}$ from Eq. (46), we find that

$$\frac{\partial \bar{G}_1}{\partial z}|_{z=0} = 0, \tag{49}$$

provided that $sJ_0'(s) \to 0$ as $s \to \infty$.

Note that from (16), we obtain

$$\begin{aligned}
\bar{G}_1|_{z=a} &= \frac{1}{2\pi D_1}\int_0^\infty \left[\exp(-\eta_1 a) + \frac{(\alpha\eta_1 - \eta_2)\exp(-\eta_1 a)\cosh(\eta_1 a)}{\alpha\eta_1\sinh(\eta_1 a) + \eta_2\cosh(\eta_1 a)}\right]\frac{\xi J_0(\xi R)}{\eta_1}d\xi, \\
\bar{G}_2|_{z=a} &= \frac{1}{2\pi D_1}\int_0^\infty \left[\exp(-\eta_2 a) + \frac{(\alpha\eta_1 - \eta_2)\exp(-\eta_2 a)\cosh(\eta_1 a)}{\alpha\eta_1\sinh(\eta_1 a) + \eta_2\cosh(\eta_1 a)}\right] \\
&\quad \times \exp[a(\eta_2 - \eta_1)]\frac{\xi J_0(\xi R)}{\eta_1}d\xi \\
&= \frac{1}{2\pi D_1}\int_0^\infty \left[\exp(-\eta_1 a) + \frac{(\alpha\eta_1 - \eta_2)\exp(-\eta_1 a)\cosh(\eta_1 a)}{\alpha\eta_1\sinh(\eta_1 a) + \eta_2\cosh(\eta_1 a)}\right]\frac{\xi J_0(\xi R)}{\eta_1}d\xi.
\end{aligned} \tag{50}$$

Consequently, $\bar{G}_1|_{z=a} = \bar{G}_2|_{z=a}$.

Now we take the partial derivative of $\bar{G}_2$ with respect to z, thereby obtaining

$$\begin{aligned}
\frac{\partial \bar{G}_2}{\partial z}|_{z=a} &= \frac{1}{2\pi D_1}\int_0^\infty \left[-\eta_2\exp(-\eta_2 a) + \frac{(\alpha\eta_1 - \eta_2)(-\eta_2)\exp(-\eta_2 a)\cosh(\eta_1 a)}{\alpha\eta_1\sinh(\eta_1 a) + \eta_2\cosh(\eta_1 a)}\right] \\
&\quad \times \exp[a(\eta_2 - \eta_1)]\frac{\xi J_0(\xi R)}{\eta_1}d\xi \\
&= \frac{1}{2\pi D_1}\int_0^\infty \left[-\eta_2 + \frac{(\alpha\eta_1 - \eta_2)[-\eta_2\cosh(\eta_1 a) - \alpha\eta_1\sinh(\eta_1 a) + \alpha\eta_1\sinh(\eta_1 a)]}{\alpha\eta_1\sinh(\eta_1 a) + \eta_2\cosh(\eta_1 a)}\right] \\
&\quad \times \exp(-a\eta_1)\frac{\xi J_0(\xi R)}{\eta_1}d\xi \\
&= \frac{1}{2\pi D_1}\int_0^\infty \left[-\eta_2 - (\alpha\eta_1 - \eta_2) + \frac{(\alpha\eta_1 - \eta_2)\alpha\eta_1\sinh(\eta_1 a)}{\alpha\eta_1\sinh(\eta_1 a) + \eta_2\cosh(\eta_1 a)}\right] \\
&\quad \times \exp(-a\eta_1)\frac{\xi J_0(\xi R)}{\eta_1}d\xi \\
&= \frac{\alpha}{2\pi D_1}\int_0^\infty \left[-1 + \frac{(\alpha\eta_1 - \eta_2)\sinh(\eta_1 a)}{\alpha\eta_1\sinh(\eta_1 a) + \eta_2\cosh(\eta_1 a)}\right] \times \exp(-a\eta_1)\xi J_0(\xi R)d\xi
\end{aligned} \tag{51}$$

On the other hand, from (45) we obtain

$$\frac{\partial \bar{G}_1}{\partial z}|_{z=a} = \frac{1}{2\pi D_1}\int_0^\infty \left[-1 + \frac{(\alpha\eta_1 - \eta_2)\sinh(\eta_1 a)}{\alpha\eta_1\sinh(\eta_1 a) + \eta_2\cosh(\eta_1 a)}\right]\exp(-\eta_1 a)\xi J_0(\xi R)d\xi \tag{52}$$

It then follows immediately that

$$\frac{\partial \bar{G}_2}{\partial z}|_{z=a} = \alpha\frac{\partial \bar{G}_1}{\partial z}|_{z=a}. \tag{53}$$

or,

$$K_1(T)\frac{\partial \bar{G}_1}{\partial z}|_{z=a} = K_2(T)\frac{\partial \bar{G}_2}{\partial z}|_{z=a}. \tag{54}$$

recalling that $\alpha = K_1(T)/K_2(T)$. The boundary condition $\bar{G}_2 \to 0$ at infinity (i.e. $z \to \infty$) is obvious.